Fast Preconditioners for Total Variation Deblurring with Anti-Reflective Boundary Conditions

Zheng-Jian Bai[*]   Marco Donatelli [†]

Stefano Serra-Capizzano [†]

October 2, 2018

Abstract

In recent works several authors have proposed the use of precise boundary conditions (BCs) for blurring models and they proved that the resulting choice (Neumann or reflective, anti-reflective) leads to fast algorithms both for deblurring and for detecting the regularization parameters in presence of noise. When considering a symmetric point spread function, the crucial fact is that such BCs are related to fast trigonometric transforms.

In this paper we combine the use of precise BCs with the Total Variation (TV) approach in order to preserve the jumps of the given signal (edges of the given image) as much as possible. We consider a classic fixed point method with a preconditioned Krylov method (usually the conjugate gradient method) for the inner iteration. Based on fast trigonometric transforms, we propose some preconditioning strategies which are suitable for reflective and anti-reflective BCs. A theoretical analysis motivates the choice of our preconditioners and an extensive numerical experimentation is reported and critically discussed. The latter shows that the TV regularization with anti-reflective BCs implies not only a reduced analytical error, but also a lower computational cost of the whole restoration procedure over the other BCs.

[*]School of Mathematical Sciences, Xiamen University, Xiamen 361005, People's Republic of China, Dipartimento di Fisica e Matematica, Università dell'Insubria - Sede di Como, Via Valleggio 11, 22100 Como, Italy, **E-mail:** zjbai@xmu.edu.cn. The research of this author was partially supported by the Natural Science Foundation of Fujian Province of China for Distinguished Young Scholars (No. 2010J06002), NCETXMU, and SRF for ROCS, SEM, and Internationalization Grant of U. Insubria 2008, 2009.

[†]Dipartimento di Fisica e Matematica, Università dell'Insubria - Sede di Como, Via Valleggio 11, 22100 Como, Italy, **E-mail:** {marco.donatelli,stefano.serrac}@uninsubria.it. The work of these authors was partially supported by MIUR, grant number 20083KLJEZ and 2006017542.

1 Introduction

We are concerned with specific linear algebra/matrix theory aspects of the vast field of inverse problems [17, 16] which model the blurring of signals and images ($2D$ or dD with $d \geq 3$). Here the goal is to reconstruct the real object from its blurred and noisy version and this goal is a classical one in astronomical imaging, medical imaging, geosciences, etc. [5].

   The blurring model is assumed to be space-invariant, i.e., the point spread function (PSF) is represented by a specific bivariate function $h(x-y)$ $(x, y \in \Omega)$ for some univariate function $h(\cdot)$ [18]. According to the linear models described in the literature [16], the observed signal or image v and the original signal or image u are described by the relation

$$v(x) = \mathcal{H}u(x) + \eta(x) := \int_{\Omega} h(x-s)u(s)ds + \eta(x), \quad x \in \Omega, \qquad (1)$$

where the kernel h is the PSF and η denotes the noise. The problem (1) is ill-posed since the operator $\mathcal{H}$ is compact [16]. Therefore, the approximation/discretization matrix of $\mathcal{H}$ is usually increasingly ill-conditioned when the number n of pixels becomes large. In addition, the size of the subspace associated with small eigenvalues, which substantially intersects the high frequencies, is large and proportional to the size of the matrix. Thus, we cannot directly solve $\mathcal{H}u = d$, since the small perturbations, represented by the noise η with important high frequency components due to its probabilistic nature, would be amplified unacceptably.

   To remedy to the latter essential ill-conditioning of problem (1), one may employ regularization methods. The Total Variation (TV) regularization approach is a good choice for restoring edges of the original signals [22]. Rudin, Osher, and Fatemi [22] gave the total variation functional in the form

$$J_{TV}(u) := \int_{\Omega} |\nabla u|\, dx, \qquad (2)$$

where $|\cdot|$ denotes the Euclidean norm. We note that the Euclidean norm $|\cdot|$ is not differentiable at zero. To avoid the non-differentiability, Acar and Vogel [2] considered the following minimization

$$\min_{u} \left\{ \|\mathcal{H}u - v\|_{L^2(\Omega)} + \alpha \int_{\Omega} \sqrt{|\nabla u|^2 + \beta^2}\, dx \right\}, \qquad (3)$$

where α, β are positive parameters. Notice that the penalty term $\int_{\Omega} \sqrt{|\nabla u|^2 + \beta^2}\, dx$ converges to $J_{TV}(u)$ as $\beta \to 0$. In other words, the latter is a differentiable regularized version of $J_{TV}(u)$. The corresponding Euler-Lagrange equation for (3)

is given by

$$\begin{cases} g(u) := \mathcal{H}^*(\mathcal{H}u - v) - \alpha\,\mathcal{L}_u(v) = 0, & x \in \Omega, \\ \qquad\qquad\qquad\qquad \frac{\partial u}{\partial n} = 0, & x \in \partial\Omega, \end{cases} \tag{4}$$

where $*$ denotes the adjoint operator and $\mathcal{L}_u(y) := -\nabla \cdot \left(\frac{1}{\sqrt{|\nabla u|^2 + \beta^2}} \nabla y \right)$ is the differential operator appearing in (4) and comes from the regularized penalty term. Vogel and Oman [29] proposed a lagged diffusivity fixed point (FP) iteration for solving (4). More precisely, given the initial guess u^0, the new iterate u^{k+1} is obtained by u^k thanks to the equation

$$A_{u^k} u^{k+1} \equiv \left(H^*H + \alpha\,L(u^k) \right) u^{k+1} = H^*v, \quad k = 0, 1, \dots, \tag{5}$$

where H and $L(u^k)u^{k+1}$ denote the discretization/approximation matrix of $\mathcal{H}$ and $\mathcal{L}_{u^k}(u^{k+1})$, respectively. We use the compound mid point rule and standard centered finite differences of precision order two for the finite dimensional approximation of $\mathcal{H}$ and $\mathcal{L}_u(\cdot)$, respectively. Therefore, at each FP iteration, we may use the preconditioned conjugate gradient (PCG) method [15, Algorithm 10.3.1] for solving the linear system (5).

In [8] the authors proposed a cosine preconditioner when H is a Toeplitz matrix, i.e., in the case of zero-Dirichlet boundary conditions (BCs). However, the choice of such BCs induces remarkable pathologies in the quality of the restored images, which should be avoided or at least minimized. In reality, using classical BCs such as periodic or zero-Dirichlet may imply, when the background is not uniformly black, disturbing Gibbs phenomena called ringing effects [20, 24, 18].

The novelty of this paper is represented by the choice of appropriate BCs, in order to reduce the ringing effects, and in the related matrix/numerical analysis. The latter will affect the algebraic expression of H, while for $L(u^k)$ the choice of the BCs in the Euler-Lagrange equation for (4) seems to impose Neumann BCs. In this context, the idea is to combine the application of anti-reflective BCs, already studied for their precision with plain regularization methods like Tikhonov and Landweber [24, 21, 26, 11, 4, 10], with the more sophisticate TV regularization. In other words, the first aim consists in checking how to reduce the ringing effects and the over-smoothing of the edges simultaneously. Next, we want to study the use of preconditioners based on innovative fast transforms in the setting of Krylov methods when the real problem is modeled by a symmetric PSF. The final goal is to combine the precision of the reconstruction with highly efficient numerical procedures. We study some preconditioning techniques and give the theoretical explanations of different proposals. An effective preconditioner for the reflective BCs is inspired by the work in [8], while, for the anti-reflective BCs, we propose a new sine preconditioner for the linear system (5) and explore the re-blurring approach introduced in [12]. Numerical results confirm the effectiveness of the proposed preconditioners and the superiority of the antireflective BCs with respect to the reflective BCs. Indeed, antireflective

BCs not only provide better restorations as expected (see [24, 11]), but also require a lower computational cost. The latter is a consequence of the fact that a more precise model requires lesser regularization, i.e. a smaller α, and the convergence of our approach is fast for small α.

The paper is organized into seven more sections. In Section 2 we consider reflective and anti-reflective BCs. Sections 3 is devoted to define optimal preconditioners for signal and image deblurring for the reflective BCs and anti-reflective BCs. In Section 4 some spectral features of the proposed preconditioners are discussed. Section 5 is concerned with the numerical tests for checking the real efficiency of the considered preconditioners and the quality of the restorations. Finally, in Section 6 we draw conclusions.

2   Boundary Conditions

We start by introducing the one-dimensional deblurring problem. Consider the original signal $\tilde{u} = (\ldots, u_{-m+1}, \ldots, u_0, u_1, \ldots, u_n, u_{n+1}, \ldots, u_{n+m}, \ldots)^T$ and the normalized blurring PSF given by

$$h = (\ldots, 0, 0, h_{-m}, h_{-m+1}, \ldots, h_0, \ldots, h_{m-1}, h_m, 0, 0, \ldots)^T, \qquad (6)$$

with the usual normalization, i.e., $\sum_{j=-m}^{m} h_j = 1$ which preserves the global intensity and therefore represents an average. The blurred signal v is the convolution of h and $\tilde{u}$ and consequently $v_i = \sum_{j=-\infty}^{\infty} h_j u_{i-j}$ is such that

$$
v = \begin{pmatrix}
h_m & \cdots & h_0 & \cdots & h_{-m} & & & & \\
 & h_m & & h_0 & & h_{-m} & & 0 & \\
 & & \ddots & \ddots & \ddots & \ddots & \ddots & & \\
 & & \ddots & \ddots & \ddots & \ddots & \ddots & & \\
 & 0 & & h_m & & h_0 & & h_{-m} & \\
 & & & h_m & \cdots & h_0 & \cdots & & h_{-m}
\end{pmatrix}
\begin{pmatrix}
u_{-m+1} \\
u_{-m+2} \\
\vdots \\
u_0 \\
u \\
u_{n+1} \\
\vdots \\
u_{n+m-1} \\
u_{n+m}
\end{pmatrix}.
$$
$$(7)$$

The deblurring problem is to recover the vector $u = (u_1, \ldots, u_n)^T$ given the blurring function h and a blurred signal $v = (v_1, \ldots, v_n)^T$ of finite length, Thus the blurred signal v is determined not only by u, but also by $(u_{-m+1}, \ldots, u_0)^T$ and $(u_{n+1}, \ldots, u_{n+m})^T$ and the linear system (7) is underdetermined. To overcome this, we make certain assumptions, that is the BCs on the unknown boundary data $u_{-m+1}, \ldots, u_0$ and $u_{n+1}, \ldots, u_{n+m}$ in such a way that the number of unknowns equals the number of equations.

For the *zero-Dirichlet* BCs, we assume that the data outside u are zero, i.e., we set $u_{1-j} = u_{n+j} = 0$ for $j = 1, \ldots, m$. Then, (7) becomes $Au = v$, where A is Toeplitz. For the *periodic* BCs, we assume that the signal u is extended by periodicity. More precisely, we set $u_{1-j} = u_{n-j+1}$ and $u_{n+j} = u_j$

for $j = 1, \ldots, m$. It follows that (7) becomes $Au = v$, where A is circulant and hence it can be diagonalized by the Discrete Fourier Transform (DFT) (see [18]).

For the *Neumann or reflective* BCs, we assume that the data outside u are a reflection of the data inside u (refer to [20]). More precisely, we set $u_{1-j} = u_j$ and $u_{n+j} = u_{n+1-j}$ for all $j = 1, \ldots, m$ in (7). Thus (7) becomes $Au = v$, where A is neither Toeplitz nor circulant but a special n-by-n Toeplitz plus Hankel matrix which is diagonalized by the discrete cosine transform provided that the blurring function h is symmetric, i.e., $h_j = h_{-j}$ for all j in (6). It follows that the above system can be solved by using three fast cosine transforms (FCTs) in $O(n \log n)$ operations [20]. This approach is computationally interesting since the FCT requires only real operations and is about twice as fast as the FFT and this is true in two dimensions as well. We note that the reflection ensures the continuity of the signal and the error is linear in the discretization step (the latter can be easily seen by applying a Taylor expansion [20]). Therefore, we usually observe a reduction of the boundary artifacts with respect to zero-Dirichlet and periodic BCs.

For the *anti-reflective* BCs, we assume that the data outside u are an anti-reflection of the data inside u. More precisely, if x is a point outside the domain and x^* is the closest boundary point, then we have $x = x^* - \delta x$ and the quantity $u(x)$ is approximated by $u(x^*) - (u(x^* + \delta x) - u(x^*))$. Consequently, we set

$$
\begin{aligned}
u_{1-j} &= u_1 - (u_{j+1} - u_1) = 2u_1 - u_{j+1}, &&\text{for all } j = 1, \ldots, m, \\
u_{n+j} &= u_n - (u_{n-j} - u_n) = 2u_n - u_{n-j}, &&\text{for all } j = 1, \ldots, m
\end{aligned}
\tag{8}
$$

in (7). By a Taylor expansion, the anti-reflection (8) ensures a C^1 continuity of the signal and the error is quadratic in the discretization step [24]. Usually, the boundary artifacts are reduced also with respect to reflective BCs.

Imposing the anti-reflection (8), the linear system (7) becomes $Au = v$, where A is a Toeplitz plus Hankel plus a rank-2 correction matrix, where the correction is placed at the first and the last column. Furthermore, in [4] the authors proved that if h is symmetric then $A = T_n \Lambda T_n^{-1}$ where

$$
T_n = \begin{bmatrix} 1 & 0 & 0 \\ p & S_{n-2} & Jp \\ 0 & 0 & 1 \end{bmatrix}, \quad T_n^{-1} = \begin{bmatrix} 1 & 0 & 0 \\ -S_{n-2}p & S_{n-2} & -S_{n-2}Jp \\ 0 & 0 & 1 \end{bmatrix},
$$

where J is the flip matrix, S_{n-2} is the sine transform matrix of order $n-2$, and where $p_j = 1 - j/(n-1)$ so that the first column vector is exactly the sampling of the function $1 - x$ on the grid $j/(n-1)$ for $j = 0, \ldots, n-1$. Finally, Λ is a diagonal matrix given by suitable samplings of the function

$$
\hat{h}(y) = \sum h_j \exp(\mathrm{i}jy),
\tag{9}
$$

which is the symbol generated by the PSF. That is,

$$
\Lambda = \mathrm{diag}_{y=1,\ldots,n} \left(\hat{h}(y_j) \right), \qquad S_m = \sqrt{\frac{2}{m+1}} \left(\sin\left(\frac{ji\pi}{m+1} \right) \right)_{i,j=1}^m,
\tag{10}
$$

5

where
$$y_j = \frac{(j-1)\pi}{n-1}, \text{ for } j = 1, \ldots, n-1, \qquad \text{and} \qquad y_n = 0. \qquad (11)$$

As a consequence, a generic system $Au = v$ can be solved within $O(n \log n)$ real operations by resorting to the application of three fast sine transforms (FSTs) (refer to [24]), where each FST is computationally as cheap as a generic FCT. There is a suggestive functional interpretation of the transform T_n. The transform associated with periodic BCs matrices is the Fourier transform: its j-th column vector, up to a normalizing scalar factor, can be viewed as a sampling, over a suitable uniform gridding of $[0, 2\pi]$, of the frequency function $\exp(-\mathbf{i}jy)$. Analogously, when imposing reflective BCs with a strongly symmetric PSF, the transform of the related reflective BCs matrices is the cosine transform: its j-th column vector, up to a normalizing scalar factor, can be viewed as a sampling, over a suitable uniform gridding of $[0, \pi]$, of the frequency function $\cos(jy)$. Here the imposition of the anti-reflective BCs, by operating a central symmetry with respect to any point of frontier, can be functionally interpreted as a linear combination of sine functions and of linear polynomials (whose use is exactly required for imposing the C^1 continuity at the borders). This intuition becomes evident in the expression of T_n. Indeed

$$T_n = \left(1 - \frac{y}{\pi}, \, \sin(y), \, \cdots, \, \sin((n-2)y), \, \frac{y}{\pi} \right) \cdot \text{diag} \left(1, \, \sqrt{\frac{2}{n-1}} I_{n-2}, \, 1 \right),$$
$$(12)$$

where y is defined (11) and it is a suitable gridding of $[0, \pi]$.

Now, we introduce the two-dimensional case. For the Neumann or reflective BCs, the blurring matrix is a block Toeplitz-plus-Hankel matrix with Toeplitz-plus-Hankel blocks and can be diagonalized by the two-dimensional FCTs (which are tensor products of one-dimensional FCTs) in $O(n^2 \log n)$ operations provided that h is quadrantally symmetric, i.e., $h_{i,j} = h_{-i,j} = h_{i,-j} = h_{-i,-j}$ (refer to [20]).

For the anti-reflective BCs, we assume that the data outside u are an anti-reflection of the data inside u, i.e., a point outside the domain is anti-reflective to the closest boundary point first in one direction and then in the other direction. In particular, we set

$$u_{1-j,\phi} = 2u_{1,\phi} - u_{j+1,\phi}, \quad u_{n+j,\phi} = 2u_{n,\phi} - u_{n-j,\phi}, \quad \text{for } 1 \le j \le m, 1 \le \phi \le n,$$
$$u_{\psi,1-j} = 2u_{\psi,1} - u_{\psi,j+1}, \quad u_{\psi,n+j} = 2u_{\psi,n} - u_{\psi,n-j}, \quad \text{for } 1 \le j \le m, 1 \le \psi \le n.$$

When both indices lie outside the range $\{1, \ldots, n\}$ (this happens close to the 4 corners of the given image), we set

$$u_{1-i,1-j} = 4u_{1,1} - 2u_{1,j+1} - 2u_{i+1,1} + u_{i+1,j+1},$$
$$u_{1-i,n+j} = 4u_{1,n} - 2u_{1,n-j} - 2u_{i+1,n} + u_{i+1,n-j},$$
$$u_{n+i,1-j} = 4u_{n,1} - 2u_{n,j+1} - 2u_{n-i,1} + u_{n-i,j+1},$$
$$u_{n+i,n+j} = 4u_{n,n} - 2u_{n,n-j} - 2u_{n-i,n} + u_{n-i,n-j},$$

for $1 \le i, j \le m$. If the blurring function (PSF) h is quadrantally symmetric, then the blurring matrix is a block Toeplitz-plus-Hankel-plus-2-rank-correction

6

matrix with Toeplitz-plus-Hankel-plus-2-rank-correction blocks and can be diagonalized by the two-dimensional anti-reflective transforms (which are tensor products of one-dimensional anti-reflective transforms T_n) in $O(n^2 \log n)$ real operations (see for instance [4]). In the following we will assume a symmetric (quadrantally symmetric in 2D) PSF since reflective and anti-reflective BCs can be diagonalized by fast transforms only in such case. However, in the nonsymmetric case, even if the blurring matrix can not be diagonalized by fast transforms, the matrix-vector product can be done again in $O(n^2 \log n)$ by FFTs. Moreover, many practical blur have the symmetry like the celebrated Gaussian blur widely used in several contexts.

3 Optimal Preconditioners with different Boundary Conditions

The optimal preconditioner for a matrix A aims to find an approximation which minimizes $\|B-A\|_F$ over all B in a set of matrices for the matrix Frobenius norm $\|\cdot\|_F$: the typical set of matrices is formed by considering an algebra of matrices which are simultaneously diagonalized by a given unitary transform. The main novelty in our context is represented by the fact that the anti-reflective matrices with symmetric PSFs form a commutative algebra associated to a non-unitary transform. The latter poses nontrivial difficulties that are treated in the sequel of the paper. The optimal circulant preconditioner was originally given in [9]. The optimal sine transform preconditioner was presented in [7]. The optimal cosine transform preconditioner was provided in [6]. In this section, we construct the optimal reflective BCs preconditioner and the optimal anti-reflective BCs preconditioner for (5) and the optimal reblurring preconditioner for the reblurring equation (20) below instead of (5). Some of these preconditioning techniques are inspired from the idea proposed in [6, 8] for zero-Dirichlet BCs.

3.1 One-dimensional Problems

For the one-dimensional problems, we assume a symmetric and normalized PSF. Suppose that we impose the reflective BCs on H and the zero Neumann BCs on $L(u^k)$. In this case, we propose the following reflective BCs preconditioners for (5). Let C_n be the n dimensional discrete cosine transform with entries

$$[C_n]_{i,j} = \sqrt{\frac{2 - \delta_{j1}}{n}} \cos\left(\frac{(2i-1)(j-1)\pi}{2n}\right), \quad i, j = 1, \ldots, n,$$

where δ_{ij} is the Kronecker delta. The matrix C_n is orthogonal, i.e., $C_n C_n^T = I$. Moreover, for any n-vector w, the matrix-vector product $C_n w$ can be computed within $O(n \log n)$ real operations by the FCT. Define

$$\mathcal{C} = \{C_n^T \Lambda C_n : \Lambda \text{ is a real } n\text{-by-}n \text{ diagonal matrix}\}.$$

For an n-by-n matrix A, the optimal cosine transform preconditioner is

$$c(A) = \operatorname*{argmin}_{B \in \mathcal{C}} \|B - A\|_F.$$

The operator $c(\cdot)$ is linear, preserves positive definiteness, and compresses every unitarily invariant norm. For the specific cosine algebra and a general convergence theory based on the Korovkin theorems, we refer to [8, 23]. As in [8] for Dirichlet BCs, the optimal cosine transform preconditioner (i.e., the optimal reflective BCs preconditioner) for (5) can be defined as

$$R = H^*H + \alpha\, c(L(u^k)). \tag{13}$$

We note that $R = c(A_{u^k})$ since $H^* = H \in \mathcal{C}$. Spectral properties of the preconditioner will be discussed in Section 4. Here, we only note that $c(L(u^k))$ is not an optimal preconditioner for $L(u^k)$ if the coefficient $(|\nabla u|^2 + \beta^2)^{-1/2}$ has large variation. In such case a diagonal scaling is necessary to obtain an effective preconditioner like $\operatorname{diag}(L(u^k))^{1/2}c(L(u^k))\operatorname{diag}(L(u^k))^{1/2}$, where $\operatorname{diag}(L(u^k))$ is the diagonal matrix whose diagonal entries are the same as that of $L(u^k)$ [25]. We note that the coefficient matrix in (5) is the sum of two operators. To avoid the possibly large fluctuation in the coefficient of the operator in (5), we define a reflective BCs preconditioner for (5) by $D_R = D^{\frac{1}{2}}RD^{\frac{1}{2}}$, where R is given in (13) and

$$D \equiv I + \alpha\, \operatorname{diag}(L(u^k)). \tag{14}$$

A further possibility is to employ a diagonal scaling for (5). As in [8], we concern the scaled equation

$$\tilde{A}_{u^k}\tilde{u}^{k+1} \equiv \left(\tilde{H}^*\tilde{H} + \alpha\, \tilde{L}(u^k)\right)\tilde{u}^{k+1} = \tilde{H}^*v, \tag{15}$$

where $\tilde{H} = HD^{-1/2}$, $\tilde{L}(u^k) = D^{-1/2}L(u^k)D^{-1/2}$, and $\tilde{u}^k = D^{1/2}u^k$. Then, we propose the following reflective BCs preconditioner for (15) $R_D = \hat{H}^*\hat{H} + \alpha\, c(\tilde{L}(u^k))$, where $\hat{H} = Hc(D^{-1/2})$. If Λ_H, Λ_D and $\Lambda_{\tilde{L}}$ denote the eigenvalue matrices of H, $c(D^{-1/2})$ and $c(\tilde{L}(u^k))$, respectively, then R_D can be written as

$$R_D = C_n^T(\Lambda_H^*\Lambda_H\Lambda_D^*\Lambda_D + \alpha\, \Lambda_{\tilde{L}})C_n.$$

Next, we construct the anti-reflective BCs preconditioners for (5) under the anti-reflective BCs for H and the Neumann BCs or anti-reflective BCs for $L(u^k)$. Let S_n be the n dimensional discrete sine transform of type I with entries as in (10). Then, S_n is orthogonal and symmetric, i.e., $S_n^T = S_n$ and $S_n^2 = I$. Moreover, for any n dimensional vector w, the matrix-vector product S_nw can be computed in $O(n \log n)$ real operations by the FST. Define $\tau = \{S_n\Lambda S_n : \Lambda \text{ is a real diagonal matrix of order } n\}$. Let $\sigma(z) := (z_2, \ldots, z_n, 0)^T$ with $z = (z_1, \ldots, z_n)^T$. Let $\mathcal{T}(z)$ be the n-by-n symmetric Toeplitz matrix whose first column is z and $\mathcal{H}(z, Jz)$ be the n-by-n Hankel matrix whose first and last column are z and Jz, respectively. It was shown that for any $B \in \tau$, there

exists $z = (z_1, \ldots, z_n)^T \in \mathbb{R}^n$ such that [7] $B = \mathcal{T}(z) - \mathcal{H}(\sigma^2(z), J\sigma^2(z))$. For an n-by-n matrix A, the optimal sine preconditioner is

$$s(A) = \operatorname*{argmin}_{B \in \tau} \|B - A\|_F. \tag{16}$$

The construction of $s(A)$ requires only $O(n^2)$ operation for a general matrix A and $O(n)$ operation for a banded matrix A. Furthermore, $s(\cdot)$ is linear, preserves positive definiteness, and compresses any unitarily invariant norm (see [7, 23]).

Now, we define an optimal sine transform based preconditioner (i.e., the so-called anti-reflective BCs preconditioner) for (5) by

$$M = \hat{s}(H)^* \hat{s}(H) + \alpha\, \hat{s}(L(u^k)) \tag{17}$$

in the sense that, for any n-by-n matrix A, $\hat{s}(A)$ is given by

$$\hat{s}(A) = \operatorname*{argmin}_{B \in \hat{\tau}} \|B - A\|_F, \tag{18}$$

where $\hat{\tau} = \left\{ \hat{S}_n \Lambda \hat{S}_n : \Lambda \text{ is a real diagonal matrix of order } n \text{ and } \hat{S}_n := \operatorname{diag}(1, S_{n-2}, 1) \right\}$.

Proposition **1** *Given an n-by-n matrix A, we have*

$$\hat{s}(A) = \begin{bmatrix} A(1,1) & 0 & 0 \\ 0 & s(A(2:n-1,2:n-1)) & 0 \\ 0 & 0 & A(n,n) \end{bmatrix}.$$

where $\hat{s}(\cdot)$ and $s(\cdot)$ are defined in (18) and (16), respectively, and $A(2:n-1,2:n-1)$ is the submatrix of A corresponding to rows indexed from 2 to $n-1$ and columns from 2 to $n-1$.

Proof: By unitary invariance of the Frobenius norm ($\hat{S}_n$ is unitary) we find $\|A - \hat{S}_n \Lambda \hat{S}_n\|_F = \|\hat{S}_n A \hat{S}_n - \Lambda\|_F$, where Λ is a diagonal matrix. To conclude the proof, it is enough to observe that

$$\operatorname{diag}(\hat{S}_n A \hat{S}_n) = \begin{bmatrix} A(1,1) & 0 & 0 \\ 0 & \operatorname{diag}(S_{n-2} A(2:n-1,2:n-1) S_{n-2}) & 0 \\ 0 & 0 & A(n,n) \end{bmatrix}.$$

and that $s(A) = S_n \operatorname{diag}(S_n A S_n) S_n$. $\qquad\square$

To reduce the potential fluctuations in the coefficient of the elliptic operator in (5), based on the diagonal scaling D in (14), we define a scaled anti-reflective BCs preconditioner for (5) by $D_M = D^{\frac{1}{2}} M D^{\frac{1}{2}}$, where M is defined in (17). Similarly, for the scaled equation in the form of (15), we give the anti-reflective BCs preconditioner with diagonal scaling as follows $M_D = \hat{H}^* \hat{H} + \alpha\, \hat{s}(\tilde{L}(u^k))$, where $\hat{H} = \hat{s}(H)\hat{s}(D^{-1/2})$. If Λ_H, Λ_D and $\Lambda_{\tilde{L}}$ denote the eigenvalue matrices of $\hat{s}(H)$, $\hat{s}(D^{-1/2})$ and $\hat{s}(\tilde{L}(u^k))$, respectively, then M_D can be written as

$$M_D = \hat{S}_n (\Lambda_H^* \Lambda_H \Lambda_D^* \Lambda_D + \alpha\, \Lambda_{\tilde{L}}) \hat{S}_n.$$

Finally, we consider the reblurring method with some new reblurring preconditioners under the anti-reflective BCs for H and the Neumann BCs for $L(u^k)$. In Section 2, we have observed that anti-reflective BCs matrices can be diagonalized by the anti-reflective transform T_n. Hence, it is possible to define the anti-reflective algebra

$$\mathcal{AR} = \{T_n \Lambda T_n^{-1} : \Lambda \text{ is a real diagonal matrix of order } n\}. \qquad (19)$$

Unfortunately, $H \in \mathcal{AR}$ but $H^* \notin \mathcal{AR}$. However, in [11], it was proposed to use a reblurring approach, i.e., to replace H^* with H', where H' is the matrix obtained by imposing anti-reflective BCs to the PSF rotated by 180 degrees. Since the PSF is assumed to be symmetric, $H' = H$ [12]. Therefore, instead of (5), one may solve the following equation [11]

$$A'_{u^k} u^{k+1} \equiv \left(H'H + \alpha\, L(u^k)\right) u^{k+1} = H'v, \quad k = 0, 1, \dots \qquad (20)$$

by the PBiCGstab method [28] since A'_{u^k} is not symmetric. In this case, a reblurring preconditioner for (20) is given by

$$P = H'H + \alpha\, AR(L(u^k)).$$

Here, for any n-by-n matrix A, $AR(A)$ is defined by

$$AR(A) := \begin{bmatrix} z_1 + 2\sum_{k=2}^{n-2} z_k & & 0 & \cdots & 0 & 0 \\ z_2 + 2\sum_{k=3}^{n-2} z_k & & & & & 0 \\ \vdots & & & & & z_{n-2} \\ z_{n-3} + 2z_{n-2} & s(A(2:n-1,2:n-1)) & & & & z_{n-3} + 2z_{n-2} \\ z_{n-2} & & & & & \vdots \\ 0 & & & & & z_2 + 2\sum_{k=3}^{n-2} z_k \\ 0 & & 0 & \cdots & 0 & z_1 + 2\sum_{k=2}^{n-2} z_k \end{bmatrix},$$

where $z = (z_1, z_2, \dots, z_{n-2})^T$ is such that $s(A(2:n-1,2:n-1)) = \mathcal{T}(z) - \mathcal{H}(\sigma^2(z), J\sigma^2(z))$. We only need form $s(A(2:n-1,2:n-1))$ for computing $AR(A)$.

We note that $AR(A)$ belongs to the algebra $\mathcal{AR}$ defined in (19), where Λ is defined as in (10). Therefore, a linear system $Au = v$ can be solved within $O(n \log n)$ real operations by using three FSTs.

Remark 2 In general, $AR(A) \neq \mathrm{argmin}_{B \in \mathcal{AR}} \|B - A\|_F$. Moreover, we can not construct $\mathrm{argmin}_{B \in \mathcal{AR}} \|B - A\|_F$ in only $O(n^2)$ operations by using the similar technique for computing $s(A)$ for a general matrix A in [6]. Notice that T_n in (12) is $T_n = \hat{S}_n(I + U)$ and $T_n^{-1} = (I - U)\hat{S}_n$, where

$$U = \begin{pmatrix} 0 & 0 & 0 \\ S_{n-2}p & 0 & S_{n-2}Jp \\ 0 & 0 & 0 \end{pmatrix}.$$

As in [19], we can compute the eigenvalue of $\mathcal{AR}(A)$ by using the diagonal entries of $\Psi = \hat{S}_n A \hat{S}_n$, However, it requires $O(n^2 \log n)$ operations to calculate the diagonal entries of Ψ.

To reduce the potential fluctuations in the coefficient of the elliptic operator in (20), we define a diagonally scaled reblurring preconditioner for (20) as follows $D_P = D^{1/2}PD^{1/2}$, where D is defined as the same form in (14). For the scaled system

$$\tilde{A}'_{u^k}\tilde{u}^{k+1} \equiv \left(\tilde{H}'\tilde{H} + \alpha\,\tilde{L}(u^k)\right)\tilde{u}^{k+1} = \tilde{H}'v, \tag{21}$$

the reblurring preconditioned is given by

$$P_D = AR(D^{-1/2})\,H'H\,AR(D^{-1/2}) + \alpha\,AR(\tilde{L}(u^k)).$$

If Λ_H, Λ_D, and $\Lambda_{\tilde{L}}$ denote the eigenvalue matrices of H, $AR(D^{-1/2})$, and $AR(\tilde{L}(u^k))$, respectively, then the preconditioner P_D can be written as

$$P_D = T_n(\Lambda_H^*\Lambda_H\Lambda_D^*\Lambda_D + \alpha\,\Lambda_L)T_n^{-1}.$$

A further possibility is the use of anti-reflective BCs for $L(u^k)$. This implies that the coefficient matrix in the linear equation (20) is closer to the preconditioner. Consequently, a faster convergence and a lower global cost have to be expected. The latter choice is in fact considered in the numerics.

We comment on the cost of constructing X_D, $X \in \{R, M, P\}$ and of each PCG/ PBiCGstab iteration. We note that $L(u^k)$ is a banded matrix. Therefore, computing $c(L(u^k))$, $\hat{s}(L(u^k))$, and $AR(L(u^k))$ needs only $O(n)$ operations [6, 7]. At each PCG/ PBiCGstab iteration, we need to calculate the matrix-vector product $\tilde{A}_{u^k}w$ and $\tilde{A}'_{u^k}w$ and solve the system $X_Dy = b$. The vector multiplication $D^{-1/2}w$ can be computed in $O(n)$ operations since $D^{-1/2}$ is a diagonal matrix. $L(u^k)w$ can be done in $O(n)$ operations. For $H \in \mathcal{C}$ or $H \in \mathcal{AR}$, Hw, H^*Hw, and $H'Hw$ can be calculated in $O(n\log n)$ operations by few FCTs or FSTs plus lower order of computations. The system $X_Dy = b$ can also be solved in $O(n\log n)$ operations. Therefore, the total cost of each PCG/ PBiCGstab iteration is bounded by $O(n\log n)$.

3.2   Two-dimensional Problems

We can extend the results in Subsection 3.1 to two-dimensional image deblurring problems with different BCs. In the two-dimensional case, we assume that the PSF is quadrantally symmetric and normalized. When one imposes the reflective BCs on H and the zero Neumann BCs on $L(u^k)$, the blurring matrix H is a block Toeplitz-plus-Hankel matrix with Toeplitz-plus-Hankel blocks, which can be diagonalized by the two-dimensional FCTs in $O(n^2\log n)$ operations [20]. For an n^2-by-n^2 matrix A in the form of

$$A = \begin{pmatrix} A_{1,1} & A_{1,2} & \cdots & A_{1,n} \\ A_{2,1} & A_{2,2} & \cdots & A_{2,n} \\ \vdots & \ddots & \ddots & \vdots \\ A_{n,1} & A_{n,2} & \cdots & A_{n,n} \end{pmatrix}, \tag{22}$$

where $A_{i,j}$ are n-by-n matrices, as defined in [8], the Level-1 cosine transform preconditioner $c_1(A)$ is given by

$$c_1(A) = \begin{pmatrix} c(A_{1,1}) & c(A_{1,2}) & \cdots & c(A_{1,n}) \\ c(A_{2,1}) & c(A_{2,2}) & \cdots & c(A_{2,n}) \\ \vdots & \ddots & \ddots & \vdots \\ c(A_{n,1}) & c(A_{n,2}) & \cdots & c(A_{n,n}) \end{pmatrix},$$

and then the Level-2 cosine transform preconditioner is $c_2(A) = Qc_1(Q^T c_1(A)Q)Q^T$, where Q be the permutation matrix which satisfies $[Q^T AQ]_{i,j;k,l} = [A]_{k,l;i,j}$ for $1 \le i, j \le n$ and $1 \le k, l \le n$, i.e., the (i,j)th entry of the (k,l)th block of A is permuted to the (k,l)th entry of the (i,j)th block.

For the two-dimensional linear equation (5), using $c_2(H) = H$, we define the optimal reflective BCs preconditioner for A_{u^k} in (5) by

$$R = H^*H + \alpha\, c_2(L(u^k)). \tag{23}$$

For eliminating the possibility of large variations in the coefficient of the elliptic operator in (5), we employ the same strategy as in Section 3.1 by the diagonal scaling in (14). Therefore, the scaled reflective BCs preconditioner is given by

$$D_R = D^{\frac{1}{2}} R D^{\frac{1}{2}}. \tag{24}$$

where R is defined in (23). Similarly, for the scaled system in (15), the reflective BCs preconditioner is given by $R_D = \hat{H}^*\hat{H} + \alpha\, c_2(\tilde{L}(u^k))$, where $\hat{H} = Hc_2(D^{-1/2})$. Let Λ_H, Λ_D and $\Lambda_{\tilde{L}}$ denote the eigenvalue matrices of H, $c_2(D^{-1/2})$ and $c_2(\tilde{L}(u^k))$, respectively. The preconditioner R_D in (24) can be written as

$$R_D = (C_n \otimes C_n)^T (\Lambda_H^* \Lambda_H \Lambda_D^* \Lambda_D + \alpha\, \Lambda_{\tilde{L}})(C_n \otimes C_n),$$

and hence it is easily inverted by employing few FCTs in $O(n^2 \log n)$ operations.

Next, we assume the anti-reflective BCs for H and the Neumann BCs or anti-reflective BCs for $L(u^k)$. Then, we construct the anti-reflective BCs preconditioners for (5). For an n^2-by-n^2 matrix A in (22), the Level-1 sine-based transform preconditioner $\hat{s}_1(A)$ is given by

$$\hat{s}_1(A) = \begin{pmatrix} \hat{s}(A_{1,1}) & \hat{s}(A_{1,2}) & \cdots & \hat{s}(A_{1,n}) \\ \hat{s}(A_{2,1}) & \hat{s}(A_{2,2}) & \cdots & \hat{s}(A_{2,n}) \\ \vdots & \ddots & \ddots & \vdots \\ \hat{s}(A_{n,1}) & \hat{s}(A_{n,2}) & \cdots & \hat{s}(A_{n,n}) \end{pmatrix}.$$

By using the same proof technique of Theorem 3.3 in [20], we can easily show that the Level-2 sine-based transform preconditioner $\hat{s}_2(A)$ is given by $\hat{s}_2(A) = Q\hat{s}_1(Q^T\hat{s}_1(A)Q)Q^T$. Notice that the matrix H is the anti-reflective BCs matrix. Then, we design the sine-based transform preconditioner for (5) by

$$M = \hat{s}_2(H)^*\hat{s}_2(H) + \alpha\, \hat{s}_2(L(u^k)).$$

By employing the diagonal scaling in (14), we define the scaled anti-reflective BCs preconditioner $D_M = D^{1/2} M D^{1/2}$ for (5) and the anti-reflective BCs preconditioner $M_D = \hat{H}^* \hat{H} + \alpha\, c_2(\tilde{L}(u^k))$, where $\hat{H} = \hat{s}_2(H)\hat{s}_2(D^{-1/2})$, for the two-dimensional system (15). Let Λ_H, Λ_D and $\Lambda_{\tilde{L}}$ denote the eigenvalue matrices of H, $\hat{s}_2(D^{-1/2})$ and $\hat{s}_2(\tilde{L}(u^k))$, respectively. Then, the preconditioner M_D takes the form

$$M_D = (\hat{S}_n \otimes \hat{S}_n)(\Lambda_H^* \Lambda_H \Lambda_D^* \Lambda_D + \alpha\, \Lambda_{\tilde{L}})(\hat{S}_n \otimes \hat{S}_n),$$

which is computationally attractive via FSTs since any matrix operation can be done within $O(n^2 \log n)$ operations.

Finally, we assume the anti-reflective BCs for H and the Neumann BCs for $L(u^k)$. For an n^2-by-n^2 matrix A defined in (22), the Level-1 reblurring preconditioner $AR_1(A)$ is given by

$$AR_1(A) = \begin{pmatrix} AR(A_{1,1}) & AR(A_{1,2}) & \cdots & AR(A_{1,n}) \\ AR(A_{2,1}) & AR(A_{2,2}) & \cdots & AR(A_{2,n}) \\ \vdots & \ddots & \ddots & \vdots \\ AR(A_{n,1}) & AR(A_{n,2}) & \cdots & AR(A_{n,n}) \end{pmatrix}.$$

Using the same proof as in [20, Theorem 3.3], we can easily show that the Level-2 reblurring preconditioner $AR_2(A)$ is given by $AR_2(A) = Q AR_1(Q^T AR_1(A)Q)Q^T$. Now, we design the reblurring preconditioner $AR_2(A'_{u^k})$ for the linear equation (20). Since H is the anti-reflective BCs matrix, we define a reblurring preconditioner for the linear equation (20) as $P = H'H + \alpha\, AR_2(L(u^k))$. Also, the reblurring preconditioner with diagonal scaling is given by $D_P = D^{1/2} P D^{1/2}$ and the reblurring preconditioner for the two-dimensional scaled linear system (21) is $P_D = \hat{H}'\hat{H} + \alpha\, AR_2(\tilde{L}(u^k))$, where $\hat{H} = H \cdot AR_2(D^{-1/2})$. Let Λ_H, Λ_D, and $\Lambda_{\tilde{L}}$ denote the eigenvalue matrices of H, $AR_2(D^{-1/2})$, and $AR_2(\tilde{L}(u^k))$, respectively. Then, the two-dimensional preconditioner P_D can be written as

$$P_D = (T_n \otimes T_n)(\Lambda_H^* \Lambda_H \Lambda_D^* \Lambda_D + \alpha\, \Lambda_{\tilde{L}})(T_n \otimes T_n)^{-1}.$$

Again, these two-dimensional preconditioner shows interesting computational features since the associated linear systems can be solved within $O(n^2 \log n)$ operations.

4 Asymptotic spectral analysis of the preconditioned sequences

In order to study the effectiveness of the proposed preconditioners, we need the clustering analysis of the spectrum. Also, localization of eigenvalues is of interest when solving (15) via PCG or (21) by PBiCGstab [1]. Here is a useful definition [25] for sequences of matrices $\{A_n\}$ where A_n has size d_n, n positive integer, and $d_k > d_q$ if $k > q$.

Definition **3** *A matrix sequence* $\{A_n\}$ *is said to be* distributed (in the sense of the eigenvalues) as the pair (θ, G), *or* have the distribution function θ, *if, for any* $F \in \mathcal{C}_0(\mathbb{C})$, *the following limit relation holds*

$$\lim_{n \to \infty} \frac{1}{n} \sum_{j=1}^{n} F\left(\lambda_j(A_n)\right) = \frac{1}{\mu(G)} \int_G F(\theta(t)) \, dt, \qquad t = (t_1, \ldots, t_d), \qquad (25)$$

where $\{\lambda_j(A_n)\}_{j=1}^{n}$ *denote the eigenvalues of* A_n *and* $\mu(\cdot)$ *is the standard Lebesgue measure. In that case we write* $\{A_n\} \sim_\lambda (\theta, G)$.

An interesting consequence of the equation (25) is that $\{A_n\} \sim_\lambda (\theta, G)$ implies that most of the eigenvalues are contained within any ϵ-neighborhood of the essential range of θ. That is, the range of θ is a cluster for the spectrum of the sequence $\{A_n\}$.

The main observation is that all the matrices considered so far are low-rank perturbations of Toeplitz matrices or can be viewed as extracted from Generalized Locally Toeplitz (GLT) sequences (see [25] and references therein and the seminal work [27]). This observation is very important since every GLT sequence has a symbol and this symbol is the spectral distribution function in the sense of the latter definition. Furthermore, the class of GLT sequences is an algebra of matrix-sequences. Hence, when making linear combinations, products, or inverses (the latter operation only when the symbol does not vanish on sets of positive measure), the result is a new GLT sequence whose symbol can be obtained via the same operations on the original symbols, as those performed on the matrices. Therefore, a particular case is that of the preconditioned matrices can be seen again as extracted from a GLT sequence whose symbol is the ratio of the symbols: here the numerator is the symbol of the original matrix sequence and the denominator is the symbol of the preconditioning sequence.

In this section, according to Definition 3 and since we are interested in asymptotic estimates, we are forced to indicate explicitly the parameter n which uniquely defines the size of the associated matrix. First, we discuss in detail the case of reflective BCs. When considering $B_n = L(u^k)$, it is well-known [25] that

$$\{B_n\} \sim_\lambda (a(x)w(t), G), \qquad G = \Omega \times [0, 2\pi]^d,$$

$$a(x) = \frac{1}{\sqrt{|\nabla x|^2 + \beta^2}} \qquad w(t) = \sum_{i=1}^{d} (2 - 2\cos(t_i)).$$

On the other hand, $c(B_n) \sim_\lambda (\overline{a}w(t), G)$, where $\overline{a}$ is a constant and in fact it is the mean of the function $a(x)$: $\overline{a} = \frac{1}{\mu(\Omega)} \int_\Omega a(x) \, dx$. The sequence $\{c(B_n)^{-1}B_n\}$ is clustered at one only if the sequence $\{B_n - c(B_n)\}$ is clustered at zero. Since $\{B_n - c(B_n)\} \sim_\lambda ((a(x) - \overline{a})w(t), G)$, the optimal cosine preconditioner is effective only if the function $a(x)$ has no large variation. To obtain a clustering preconditioner, a diagonal scaling has to be introduced. Indeed, the preconditioner $\text{diag}(B_n)^{1/2}c(B_n)\text{diag}(B_n)^{1/2}$ is such that $\{\text{diag}(B_n)^{1/2}c(B_n)\text{diag}(B_n)^{1/2}\} \sim_\lambda (a(x)w(t), G)$ due to the algebra stucture

of GLT sequences, and hence the preconditioned sequence is clustered at one. In our case, the coefficient matrix

$$A_n = H^*H + \alpha L(u^k)$$

is the sum of an integral approximate operator and an approximate elliptic differential operator. We note that $\{A_n\} \sim_\lambda (|\hat{h}(t)|^2 + \alpha a(x)w(t), G)$, where $\hat{h}$ is the symbol of the PSF defined in (9) for the 1D case and similarly can be defined for $d > 1$ (the entries of the PSF are the Fourier coefficients of $\hat{h}$). An effective preconditioner has to consider both terms which consitute the matrix A_n. This is the aim of the preconditioner R_n defined in (13) and (23) for the 1D and 2D case, respectively. We have $\{R_n\} \sim_\lambda (|\hat{h}(t)|^2 + \alpha \overline{a} w(t), G)$ and so $\{A_n - R_n\} \sim_\lambda ((a(x) - \overline{a})\alpha w(t), G)$. In this case, we can not apply a diagonal scaling to $c(L(u^k))$ because otherwise we loose the computational efficiency, the matrix $H^*H + \alpha \text{diag}(L(u^k))^{1/2} c(L(u^k)) \text{diag}(L(u^k))^{1/2}$ can not be diagonalized by discrete cosine transforms. Therefore, we have to apply to R_n a diagonal scaling which should be act like $\text{diag}(L(u^k))^{1/2}$ on $c(L(u^k))$, while it should be no affect the term H^*H. Unfortunately, since we have a diagonal scaling we can not apply the diagonal scaling only to a term of the sum. To balance the contribution of the two terms, the diagonal scaling is defined by the matrix D in (14) which leads to the preconditioner D_R. We have $\{(D_R)_n\} \sim_\lambda ((1 + \alpha a(x))(|\hat{h}(t)|^2 + \alpha w(t)), G)$ and hence the preconditioned sequence is not clustered at one, even if for values of α used in the considered applications it shows an optimal behaviour (see Figure 2). We recall that the clustering is a useful property but it is not strictly necessary for the optimality of the related preconditioned Krylov method: for instance in the Hermitian positive definite case and when dealing with the PCG iterations, the spectral equivalence is sufficient. Since $D_R^{-1} A_n$ is similar to $R^{-1} \tilde{A}_n$, with $\tilde{A}_n = D^{-1/2} A_n D^{-1/2}$, the use of the preconditioner D_R to the linear system (5) is equivalent to apply the preconditioner R to the scaled linear system (15). However, the scaling of the linear suggest to use a cosine preconditioner different from R that is R_D which is more effective for large values of α (see numerical results in Section 5).

*Remark **4** For small values of α, i.e., when few regularization is required, the three preconditioners R, D_R and R_D have a similar behaviour. Moreover, when α goes to zero the effectiveness of the proposed preconditioners increases because the preconditioners and the original coefficient matrix A_n all tend to H^*H.*

For concluding this section, we note that in the case of anti-reflective BCs similar considerations can be done. The main difference is when we consider the reblurring strategy. However, using the results in [14], the nonsymmetric case can be considered as well since the antisymmetric part has trace norm (sum of all singular values) bounded by a pure constant independent of n. Therefore the spectral distribution is governed by the symmetric part which is dominant as discussed in Section 3.3 of [3].
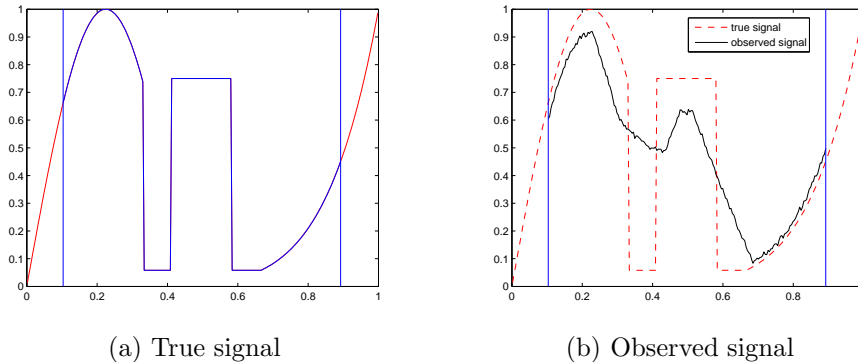
(a) True signal　　　　　　　　　(b) Observed signal

Figure 1: True and observed signals

5　Numerical Tests

We will solve the problem (4) by the fixed point method (5) with the operator $\mathcal{H}$ approximated by using different BCs and with the matrix $\mathcal{L}$ imposed by zero Neumann BCs or anti-reflective BCs. The algorithm was implemented in `MATLAB` `7.10` and run on a PC Intel Pentium IV of 3.00 GHZ CPU. We shall show the effectiveness of the proposed preconditioners for the signal/image deblurring and also give a comparison of the quality of the restored signals/images with different BCs.

In our test, for simplicity, we choose initial guess $u^0 = v$ for the FP algorithm. We shall solve (5) by the PCG method when the Neumann BCs imposed on $L(u^k)$ and solve (5) by the PBiCGstab method when the anti-reflective BCs imposed on $L(u^k)$. Also, we solve (20) by the PBiCGstab method. The initial guess for the PCG and PBiCGstab methods in kth FP iteration is chosen to be the $(k-1)$th FP iterate. The PCG and PBiCGstab iterations are stopped when the residual vector r_k of the linear systems (5) and (20) at the kth iteration satisfies $\|r_k\|_2/\|r_0\|_2 < tol$, where tol is set to 10^{-6} and 10^{-5} in the 1D and 2D case, respectively.

5.1　1D case: Signal Deblurring

In our experiments, we suppose the true signal u is given as in Figure 1(a). The two vertical lines shown in Figure 1(a) denote the field of view (i.e., $[0.1, 0.9]$) of our signal and the signal outside the two vertical lines can be approximated by different BCs. The true signal is blurred by the symmetric out of focus PSF:

$$h_i = \begin{cases} c & \text{if } |i| < m(n), \\ 0 & \text{otherewise,} \end{cases} \tag{26}$$

where c is the normalization constant such that $\sum_i h_i = 1$ and $m(n)$ is the center of the PSF which depends on n so that the restored signal lies in the

PCG	R						AR+Sine+ZN $\mathcal{L}$					
α	N	I	D	R	D_R	R_D	N	I	D	M	D_M	M_D
10^{-1}	30	269	163	73	49	45	28	221	155	60	51	36
10^{-2}	37	172	107	84	37	32	24	149	94	67	33	25
10^{-3}	32	99	71	63	42	36	24	80	59	56	37	31
10^{-4}	19	57	56	38	36	35	19	60	58	31	30	29
10^{-5}	20	74	71	23	25	24	17	47	45	20	20	19
10^{-6}	11	122	122	7	7	8	8	85	86	14	14	14

PBiCGstab	AR+Reblur+ZN $\mathcal{L}$						AR+Reblur+AR $\mathcal{L}$					
α	N	I	D	P	D_P	P_D	N	I	D	P	D_P	P_D
10^{-1}	27	178	105	57	53	51	24	179	109	41	46	35
10^{-2}	24	105	59	59	25	21	23	107	60	39	23	20
10^{-3}	23	60	44	43	27	23	22	54	37	34	22	20
10^{-4}	20	33	31	20	18	18	20	32	30	18	16	17
10^{-5}	25	31	33	10	9	10	20	31	32	10	10	10
10^{-6}	9	78	68	4	4	4	11	56	62	4	4	4

Table 1: Average number of PCG/PBiCGstab iterations per FP step varying α, with $n = 203$ and $\beta = 0.1$.

interval $[0.1, 0.9]$. A Gaussian noise η with noise-to-signal ratio $\|\eta\|_2/\|Hu\|_2$ is added to the blurred signal. We consider the true signal is blurred by the out of focus PSF and then added the Gaussian noise with the noise levels 1%, i.e., $\|\eta\|_2/\|Hu\|_2 = 0.01$. Figure 1(b) show the observed signal.

We now show that the proposed preconditioners are effective for solving (5) and (20) with different BCs. In our numerical experiment, the FP iteration is stopped when $\|u^k - u^{k-1}\|_2/\|u^k\|_2 < 10^{-3}$. We will concentrate on the performance of different choices of preconditioners for various of parameters α, β, and n.

In Tables 1 and 2, we report the average number of iterations per FP iteration, where N, I and D denote the number of FP steps, no preconditioner and the diagonal scaling preconditioner, respectively. According to Remark 4, the effectiveness of the proposed preconditioners increases when α decreases. Moreover, decreasing α all the proposed preconditioners become equivalents, explicitly the PCG/PBiCGstat converges in about the same number of iterations.

We note that anti-reflective BCs usually require lesser steps and lesser PCG/BiCGstab iterations per FP step when compared with reflective BCs. This shows that the improvement in the model also leads to an improvement in the global computational complexity of the numerical methods. This is more evident for the optimal restoration since antireflective BCs require a regularization parameter α smaller than the reflective BCs (Figures 4–5).

Figure 2 describes the average PCG/PBiCGstab iterations per FP step vary-

PCG	R						AR+Sine+ZN $\mathcal{L}$					
β	N	I	D	R	D_R	R_D	N	I	D	M	D_M	M_D
10^{-3}	31	434	245	305	298	125	24	349	200	297	226	85
10^{-2}	31	218	139	149	98	67	24	175	112	139	72	46
10^{-1}	32	99	71	63	42	36	24	80	59	56	37	31
10^{0}	28	39	36	21	18	20	21	35	32	19	16	15

PBiCGstab	AR+Reblur+ZN $\mathcal{L}$						AR+Reblur+AR $\mathcal{L}$					
β	N	I	D	P	D_P	P_D	N	I	D	P	D_P	P_D
10^{-3}	23	403	254	361	346	59	22	323	207	288	285	57
10^{-2}	23	157	87	130	58	43	22	134	77	102	43	28
10^{-1}	23	60	44	43	27	23	22	54	37	34	22	20
10^{0}	20	21	20	12	11	11	20	19	18	10	9	9

Table 2: Average number of PCG/PBiCGstab iterations per FP step varying β, with $n = 203$ and $\alpha = 0.001$.

ing n. We note that the preconditioners with a diagonal scaling show an optimal behavior.

In Figure 3, we present the restored signals for varying β, e.g., by solving system (5) when anti-reflective BCs have been imposed. As expected, the recovered signals become shaper when the value of β is smaller, the value $\beta = 0.1$ gives a restoration sufficiently good anyway.

We can easily observe from Tables 1-2 and Figure 2 that the proposed preconditioners with a diagonal scaling are the most effective preconditioner when varying parameters α, β, and n. Finally, we remark that in all our tests, the proposed algorithm needs the same number of FP steps for the no-preconditioner and preconditioned cases and $\|g(u^k)\|_2$ tends to $O(10^{-5})$ or $O(10^{-6})$ at the final FP iterate.

To check the quality of restored signals by using different BCs, in Figure 4 we show the relative restoration error (RRE), $\|u_\alpha - u\|_2/\|u\|_2$, where u_α is the total variation regularized solution of the true signal u, versus the regularization parameter α. Figure 5 gives the restored signals with optimal value of the parameter α, where $\alpha_{\tt opt}$, $\tt Re.$, $\tt Fp.$, and $\tt It.$ denote the optimal value of the parameter α, the minimal RRE, the number of FP steps, and the average number of PCG/BiCGstab iterations per FP step, respectively.

From Figure 5 we argue that anti-reflective BCs lead to the most accurate restored signals with less significant ringing effects at the edges and less PCG iterations per FP step, when compared with reflective BCs. Moreover, thanks to the improvement in the model of the problem, antireflective BCs require lesser regularization than reflective BCs. This implies a smaller $\alpha_{\tt opt}$ and hence a small number of PCG/BiCGstab iterations per FP step, while the number of FP iterations remains about the same.
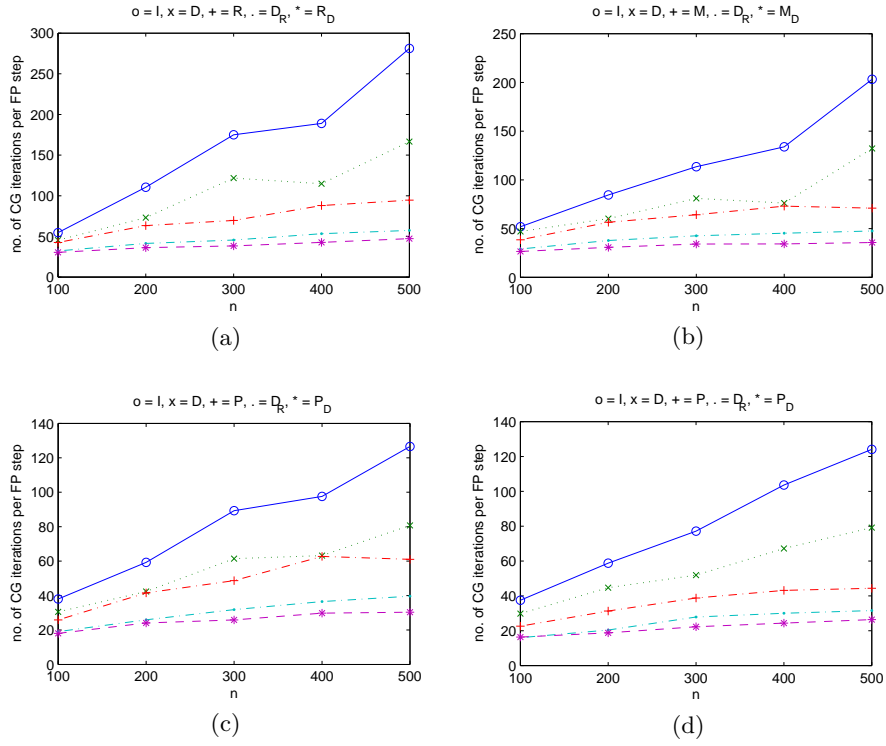
Figure 2: Average number of PCG/PBiCGstab iterations per FP step for various n, with $\alpha = 10^{-3}$ and $\beta = 0.1$. (a) Reflective BCs. (b) Anti-Reflective BCs with sine preconditioner. (c) Anti-Reflective BCs with reblurring by imposing zero Neumann BCs on $\mathcal{L}$. (d) Anti-Reflective BCs with reblurring by imposing Anti-Reflective BCs on $\mathcal{L}$.
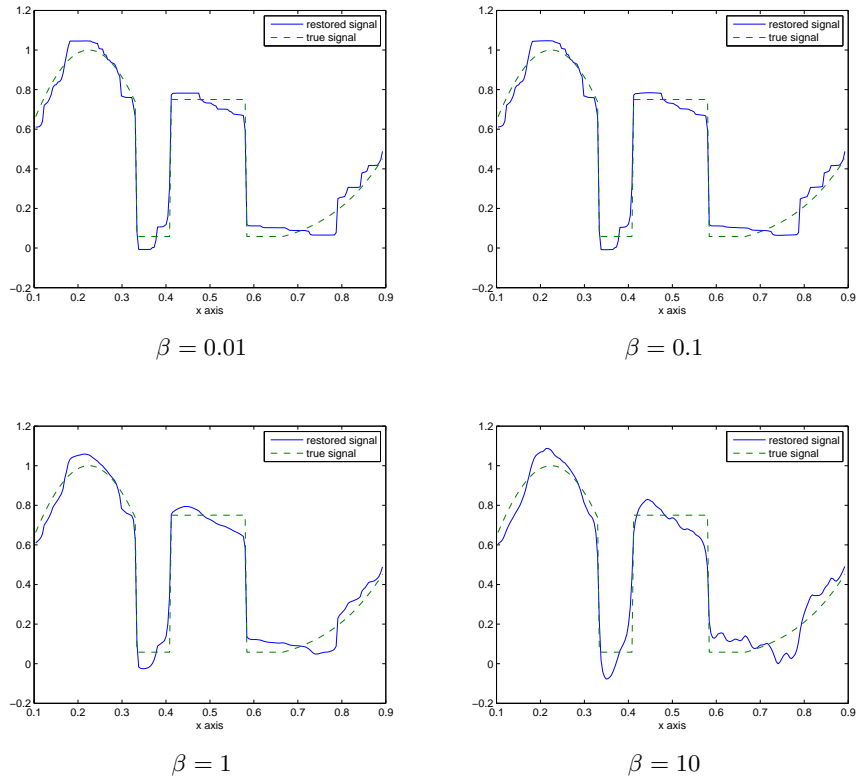
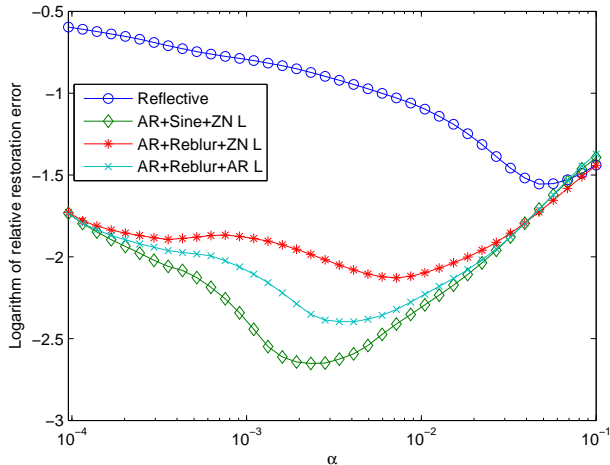Figure 3: Restorations for Anti-Reflective BCs based (5) with $n = 203$, $\alpha = 10^{-3}$ varying β.

Figure 4: The RRE versus the regularization parameter α for different BCs.

5.2   2D case: Image Deblurring

In this section, we apply the proposed preconditioners to image restoration with different BCs. Suppose the true images are blurred by the Gaussian blur and then suppose that a white Gaussian noise η with the noise levels 0.1% is added. Figure 6 shows the true and observed images.

In our numerical tests, the FP iteration is stopped when $\|u^k - u^{k-1}\|_2/\|u^k\|_2 < 10^{-4}$ and the maximal number of FP steps is set to be 100. We fix $\beta = 0.01$ and only focus on the performance of different choices of preconditioners for varying α.

In Table 3 the number of iterations is displayed for solving (5) and (20) with different BCs and various values of α, where N and I mean the number of FP iterations and no preconditioner, respectively. Here, we only give the average number of CG/BiCGstab iterations per FP step. Table 3 suggests that the preconditioners X_D, with $X \in \{R, M, P\}$, are very effective matrix approximations for all values of α, while the preconditioners D_X do not work well for large values of α especially for antireflective BCs. However, for antireflective BCs a good choice for α is in the interval $[10^{-3}, 10^{-2}]$ and in this case both choices X_D and D_X have a similar behaviour. We note that the number of FP iterations decrease with α, so if we have a good model that requires a lower regularization we obtain a gain also in terms of the computational cost of the whole restoration procedure. In all our tests, it is shown that $\|g(u^k)\|_2$ tends to $O(10^{-3})$ or $O(10^{-4})$ at the final FP iterate.

Next, we shall check the quality of restored images by using different BCs. Figure 7 describes the relative restoration error (RRE) $\|u_\alpha - u\|_2/\|u\|_2$ versus the regularization parameter α. Figure 8 presents the restored images with
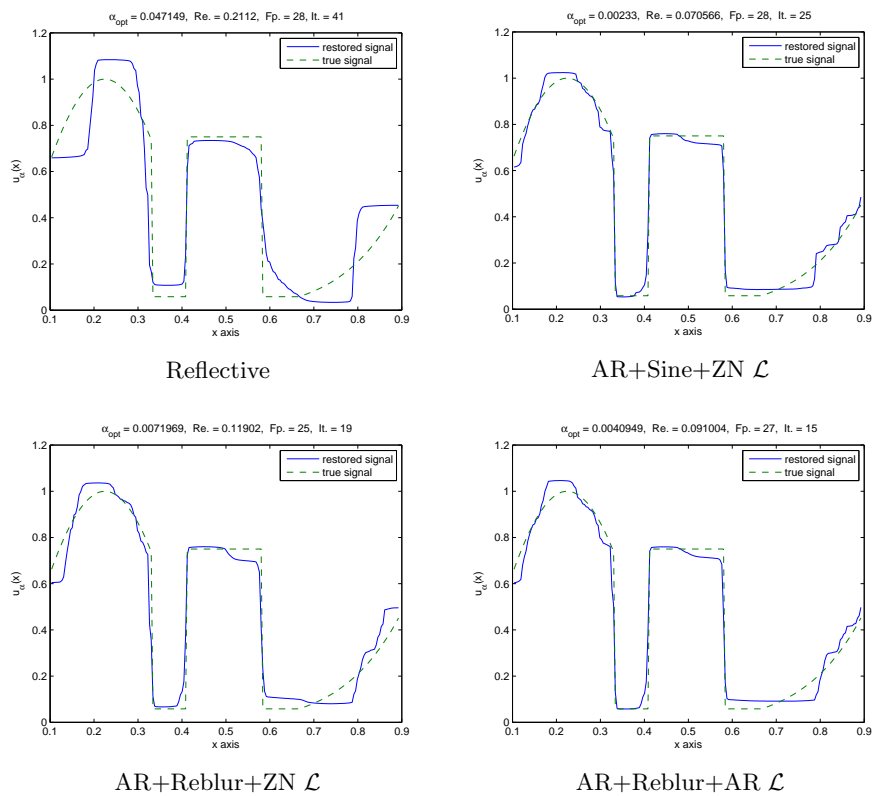
Figure 5: Restored signals with different BCs. Here $n = 203$ and $\beta = 0.1$

Figure 6: True and observed images

PCG			R						AR+Sine+ZN $\mathcal{L}$		
α	N	I	N	D_R	N	R_D	N	I	N	D_M	N	M_D
10^0	60	244	60	48	60	23	60	229	60	210	61	23
10^{-1}	41	129	46	29	33	22	40	114	40	117	28	38
10^{-2}	13	70	13	44	11	39	12	58	9	49	8	41
10^{-3}	3	124	2	42	2	42	2	147	2	36	2	37
10^{-4}	2	164	1	23	1	23	1	354	1	23	1	23

PBiCGstab			AR+Reblur+ZN $\mathcal{L}$						AR+Reblur+AR $\mathcal{L}$		
α	N	I	N	D_P	N	P_D	N	I	N	D_P	N	P_D
10^0	58	52	$*$	$*$	59	13	60	52	59	50	60	7
10^{-1}	27	27	33	16	31	7	26	28	31	9	30	5
10^{-2}	10	9	10	7	10	6	10	10	12	5	10	5
10^{-3}	2	16	2	5	2	5	3	11	2	4	2	5
10^{-4}	1	33	1	3	2	1	1	34	1	3	2	1

Table 3: Average number of CG/BiCGstab iterations per FP step for varying α. Here, $\beta = 0.01$ ($*$ means that the method does not converge).
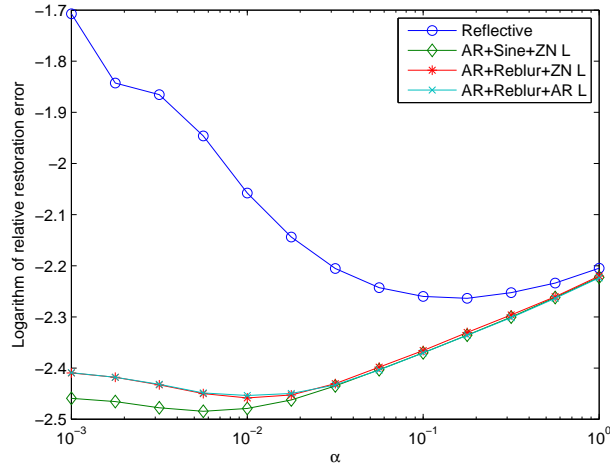
Figure 7: The RRE versus the regularization parameter α for different BCs.

α_{opt} = 0.17783, Re. = 0.10398, Fp. = 37, It. = 22

$\alpha_{opt} = 0.17783$, Re. = 0.10398, Fp. = 37, It. = 22

$\alpha_{opt} = 0.0056234$, Re. = 0.083353, Fp. = 6, It. = 35

Reflective

AR+Sine+ZN $\mathcal{L}$

$\alpha_{opt} = 0.01$, Re. = 0.085559, Fp. = 8, It. = 16

$\alpha_{opt} = 0.01$, Re. = 0.085984, Fp. = 8, It. = 14

AR+Reblur+ZN $\mathcal{L}$

AR+Reblur+AR $\mathcal{L}$

Figure 8: Restored images with different BCs.

optimal value of the parameter α. Like in the 1D case, Figure 8 shows that the anti-reflective BCs lead to better restored images and shaper edges with a lower computational cost than the reflective BCs (note the high reduction in the FP iterations being α_{opt} smaller).

6   Conclusions

In this paper, we have considered the effect of reflective and anti-reflective BCs, when regularizing blurred and noisy images via the total variation approach. In particular, we have studied some preconditioning strategies for the linear systems arising from the FP iteration given in [29]. In the case of anti-reflective BCs we have also considered a comparison with the reblurring idea proposed in [12]. We recall that the latter has been shown effective when combined with the Tikhonov regularization and here one of the issues was to verify that reblurring and total variation can be combined satisfactorily. Furthermore, the optimal behavior of our preconditioners has been validated numerically.

Beside the computational features of the preconditioning techniques, we stress the improvement obtained via anti-reflective BCs both in terms of reconstruction quality and reduction of the computational cost. In fact, the precision of such BCs was already known in the relevant literature (see [11, 10, 21] and references there reported). However, this is the first time that the anti-reflective BCs have been combined with a sophisticated regularization method, where the use of fast transforms is very welcome for saving computational cost. The precision of the antireflective BCs implies also a further reduction of the computational cost over the other BCs (see numerical results in Section 5) because they require a smaller regularization parameter α and the effectiveness of the proposed preconditioners increases reducing α.

Potential lines of interest for future investigations could include the use of anti-reflective BCs in the promising split Bregman method recently proposed in [13] and a more precise clustering analysis of the preconditioning sequences, in the spirit of Section 4.

References

[1] O. Axelsson and G. Lindskog, *On the rate of convergence of the preconditioned conjugate gradient method*, Numer. Math. 48 (1986), pp. 499–523.

[2] R. Acar and C. Vogel, *Analysis of total variation penalty methods*, Inverse Problems, 10 (1994), pp. 1217–1229.

[3] A. Aricó, M. Donatelli, and S. Serra-Capizzano, *Spectral analysis of the anti-reflective algebras and applications*, Linear Algebra Appl., 428/2-3 (2008), pp. 657–675.

[4] A. Aricó, M. Donatelli, J. Nagy, and S. Serra-Capizzano, *The anti-reflective transform and regularization by filtering*, special volume Numerical Linear

Algebra in Signals, Systems, and Control., in Lecture Notes in Electrical Engineering, Springer Verlag, in press.

[5] M. Bertero and P. Boccacci, *Introduction to Inverse Problems in Imaging*, Inst. of Physics Publ. London, UK, 1998.

[6] R. Chan, T. Chan, and C. Wong, *Cosine transform based preconditioners for total variation minimization problems in image processing*, in Proc. 2nd IMACS Int. Symp. Iterative Methods in Linear Algebra Iterative Methods in Linear Algebra, II, V3, IMACS Series in Computational and Applied Mathematics, S. Margenov and P. Vassilevski, Eds., June 1995, pp. 311–329.

[7] R. Chan, M. Ng, and C. Wong, *Sine transform based preconditioners for symmetric Toeplitz systems*, Linear Algebra Appl., 232 (1996), pp. 237–259.

[8] R. Chan, T. Chan, and C. Wong, *Cosine transform based preconditioners for total variation deblurring*, IEEE Trans. Image Proc., 8 (1999), pp. 1472–1478.

[9] T. Chan, *An optimal circulant preconditioner for Toeplitz systems*, SIAM J. Sci. Statist. Comput. 9 (1988), pp. 766–771.

[10] M. Christiansen and M. Hanke, *Deblurring methods using antireflective boundary conditions*, SIAM J. Sci. Comput., 30 (2008), pp. 855–872.

[11] M. Donatelli, C. Estatico, and S. Serra-Capizzano, *Improved image deblurring with anti-reflective boundary conditions and re-blurring*, Inverse Problems, 22 (2006), pp. 2035–2053.

[12] M. Donatelli and S. Serra Capizzano, *Anti-reflective boundary conditions and re-blurring*, Inverse Problems, 21 (2005), pp. 169–182.

[13] T. Goldstein, S. Osher, *The split Bregman method for L1-regularized problems*, SIAM J. Imaging Sci. 2 (2009), pp. 323–343.

[14] L. Golinskii and S. Serra-Capizzano, *The asymptotic properties of the spectrum of nonsymmetrically perturbed Jacobi matrix sequences*, J. Approx. Theory, 144 (2007) pp. 84–102,

[15] G. Golub and C. Van Loan, *Matrix Computations*, 3rd edition, Johns Hopkins University Press, Baltimore and London, 1996.

[16] C. Groetsch, *Inverse Problems in the Mathematical Sciences*, Wiesbaden, Germany, Vieweg, 1993.

[17] H. Engl, M. Hanke, and A. Neubauer, *Regularization of Inverse Problems*, Kluwer Academic Publishers, Dordrecht, The Netherlands, 1996.

[18] P. C. Hansen, J. Nagy, and D. P. O'Leary, *Deblurring Images Matrices, Spectra and Filtering*, SIAM Pulications, Philadelphia, 2005.

[19] T. Huckle, *Circulant and skew circulant matrices for solving Toeplitz matrix problems*, SIAM J. Matrix Anal. Appl., 13 (1992), pp. 767–777.

[20] M. Ng, R. Chan, and W. Tang, *A fast algorithm for deblurring models with Neumann boundary conditions*, SIAM J. Sci. Comput., 21 (1999), pp. 851–866.

[21] L. Perrone, *Kronecker product approximations for image restoration with anti-reflective boundary conditions*, Numer. Linear Algebra Appl., 13 (2006), pp. 1–22.

[22] L. Rudin, S. Osher, and E. Fatemi, *Nonlinear total variation based noise removal algorithms*, Physica D., 60 (1992), pp. 259–268.

[23] S. Serra Capizzano, *A Korovkin-type Theory for finite Toeplitz operators via matrix algebras*, Numer. Math., 82 (1999), pp. 117–142.

[24] S. Serra Capizzano, *A note on antireflective boundary conditions and fast deblurring models*, SIAM J. Sci. Comput., 25 (2003), pp. 1307–1325.

[25] S. Serra-Capizzano, *The GLT class as a Generalized Fourier Analysis and applications*, Linear Algebra Appl., 419 (2006), pp. 180–233.

[26] Y. Shi and Q. Chang, *Acceleration methods for image restoration problem with different boundary conditions*, Applied Numer. Math., 58 (2008), pp. 602–614.

[27] P. Tilli, *Locally Toeplitz sequences: spectral properties and application*, Linear Algebra Appl., 278 (1998), pp. 91–120.

[28] H. van der Vorst, *BI-CGSTAB: A fast and smoothly converging variant of BI-CG for the solution of nonsymmetric linear systems*, SIAM J. Sci. Stat. Comput., 13 (1992), pp. 631–644.

[29] C. Vogel and M. Oman, *Iterative methods for total variation denoising*, SIAM J. Sci. Comput., 17 (1996), pp. 227–238.

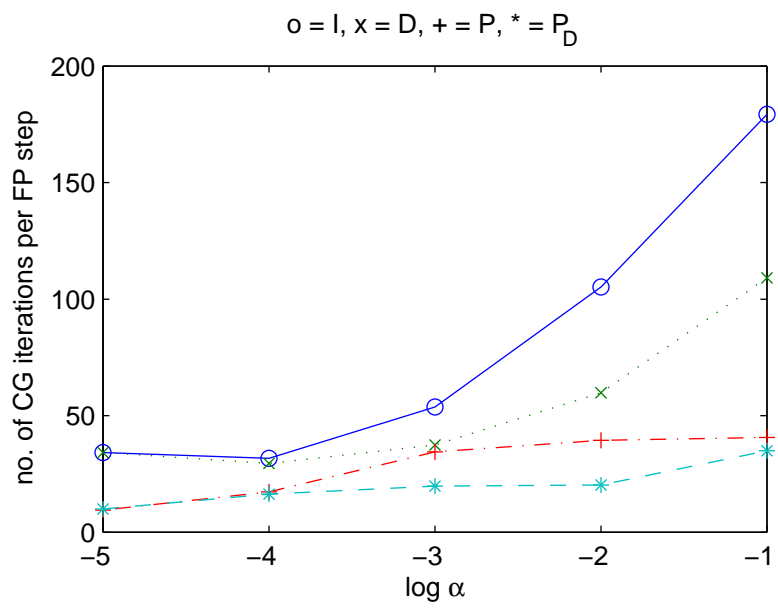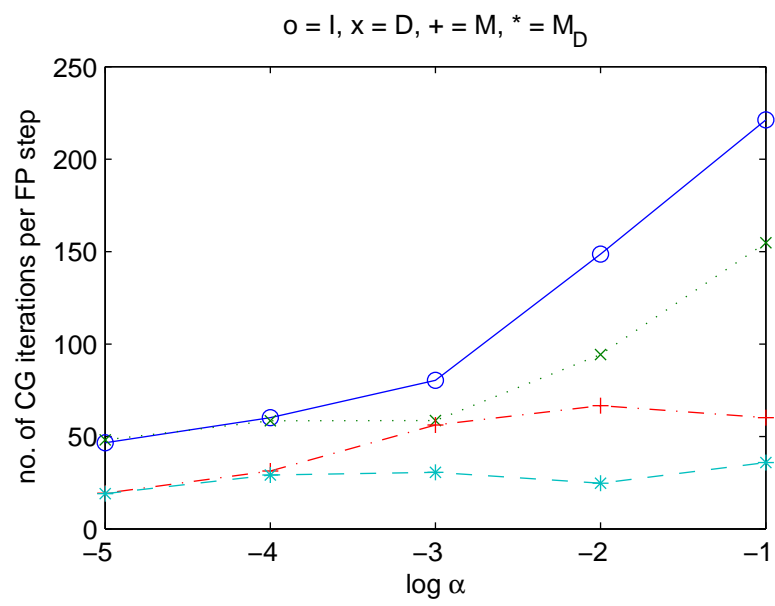$\alpha_{opt} = 0.00233$, Re. = 0.071501, Fp. = 28, It. = 18
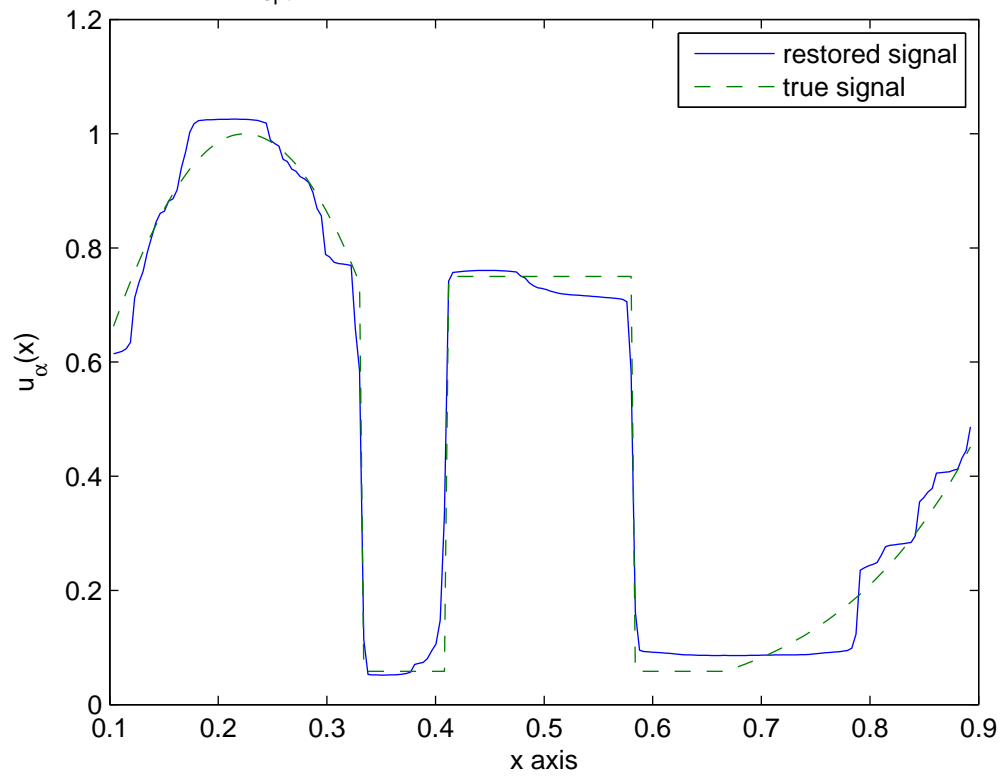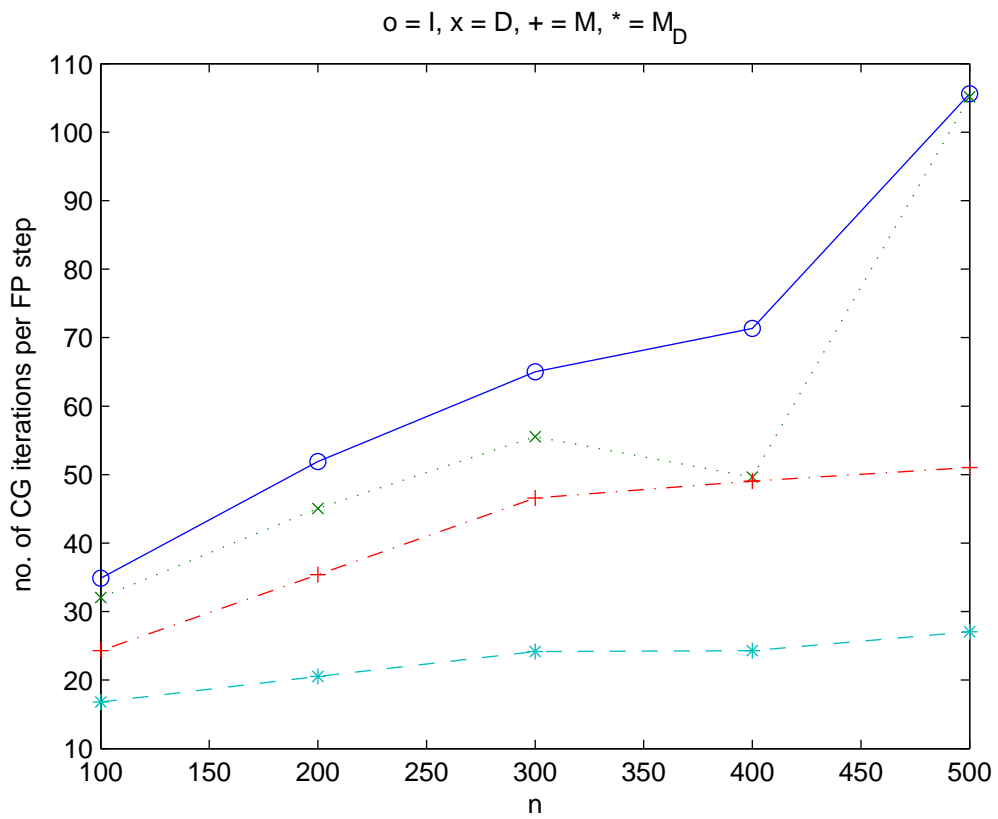
$\alpha_{opt} = 0.01$, Re. = 0.085556, Fp. = 9, It. = 23

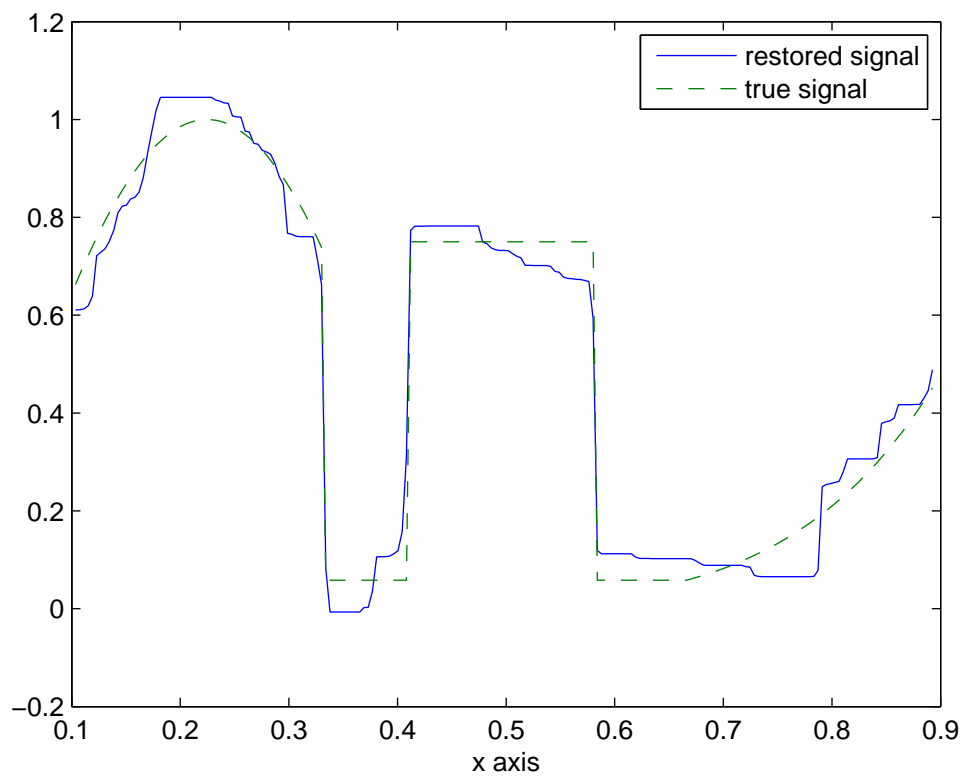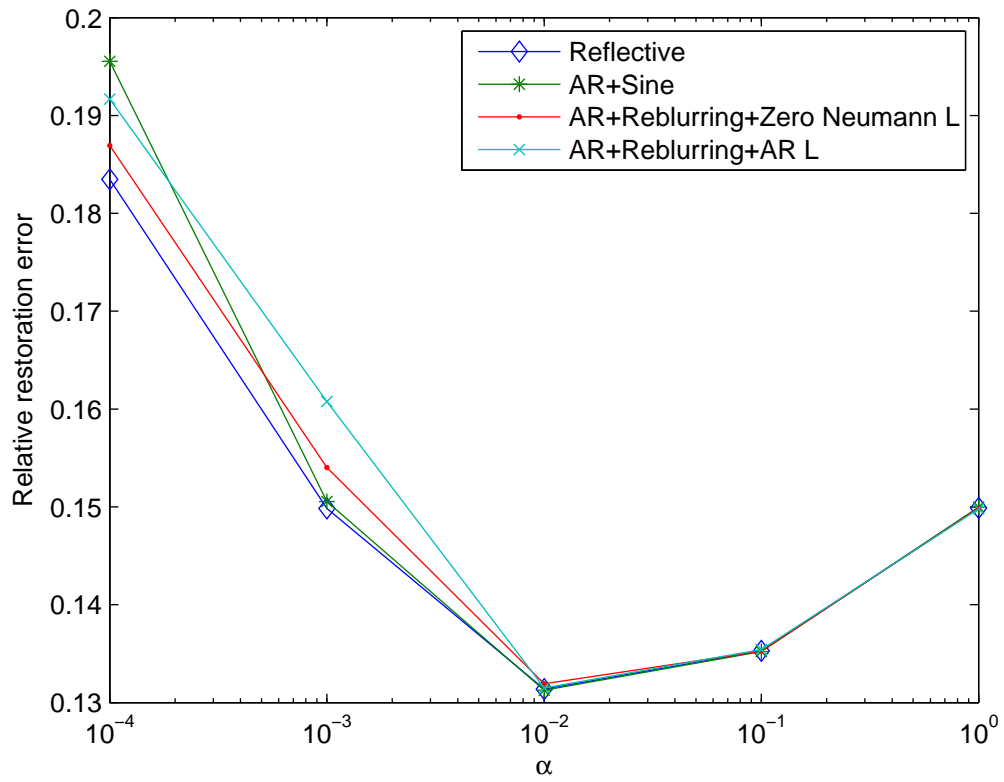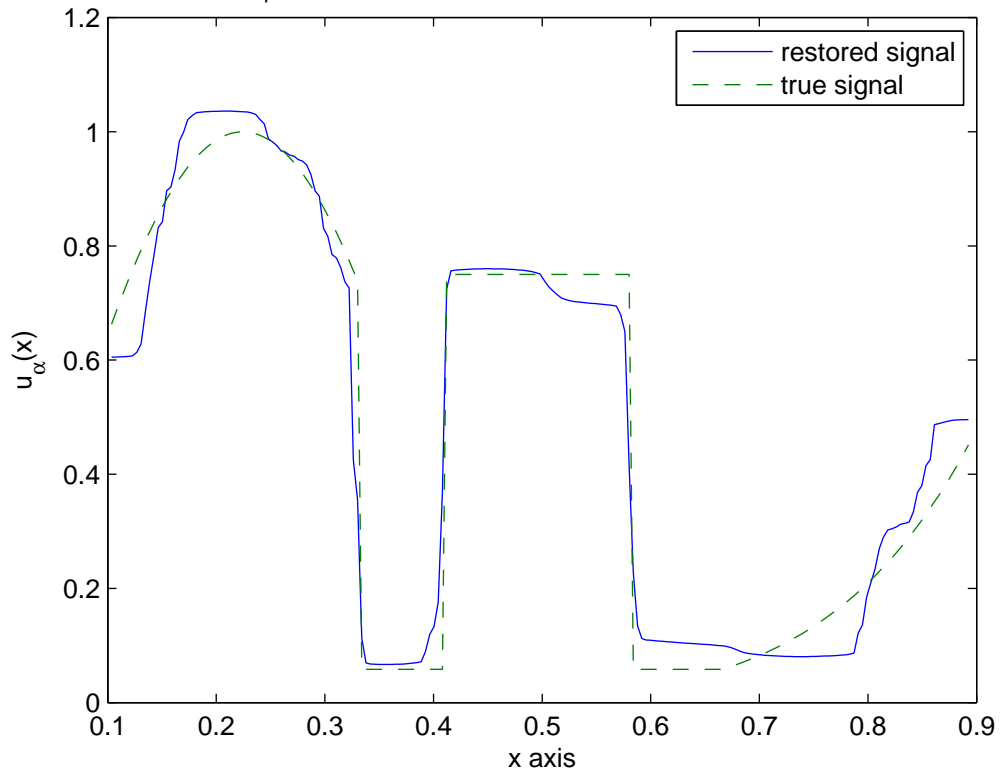$o = I, x = D, + = M, * = M_D$
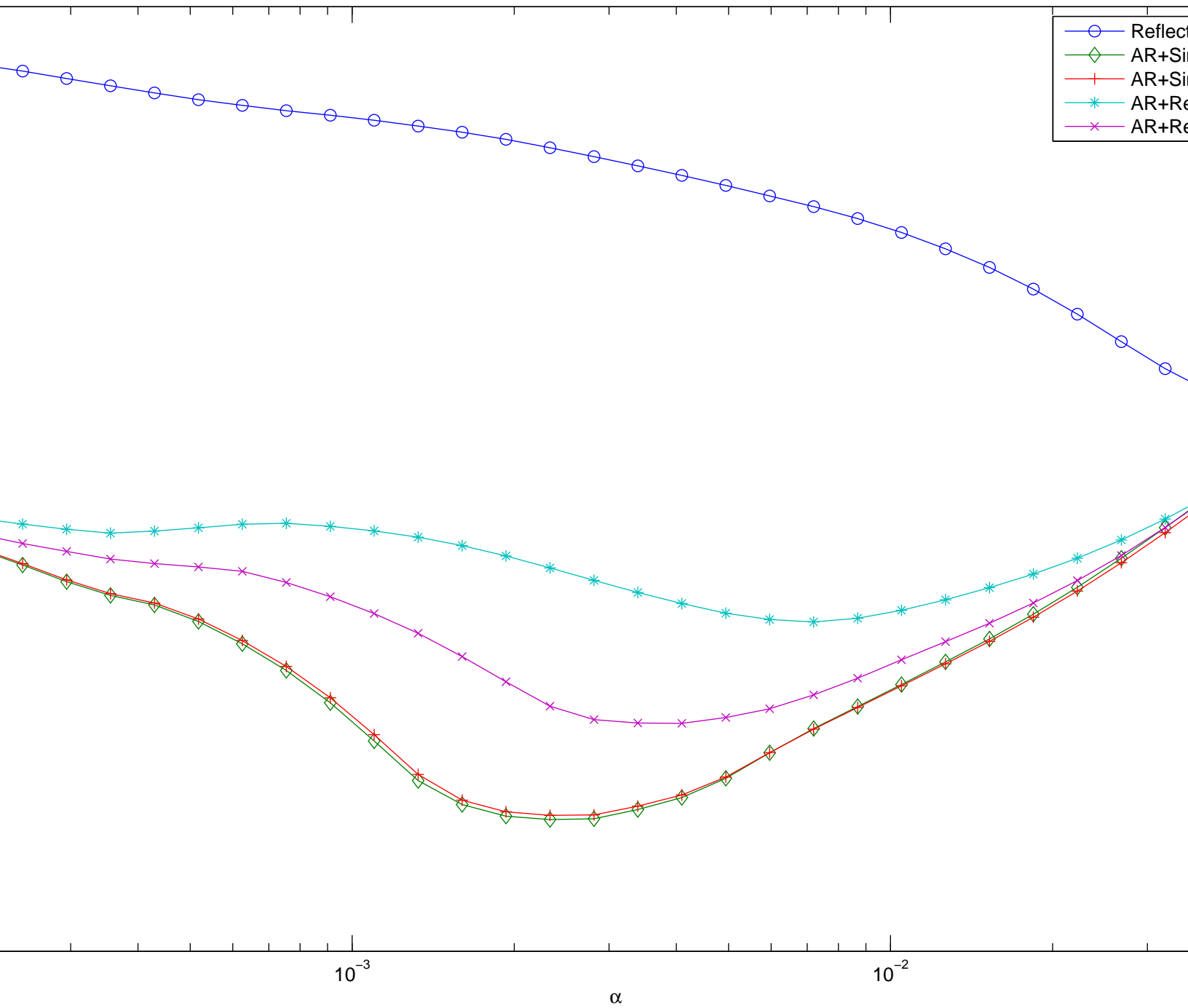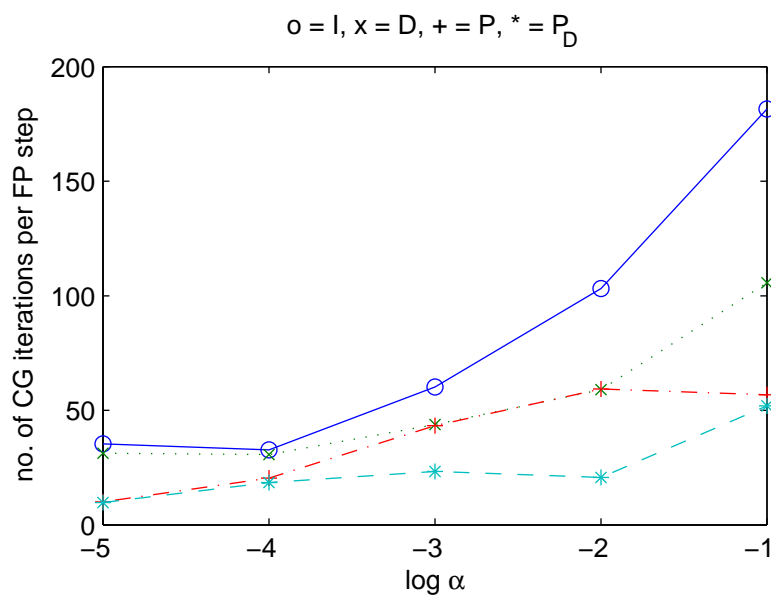
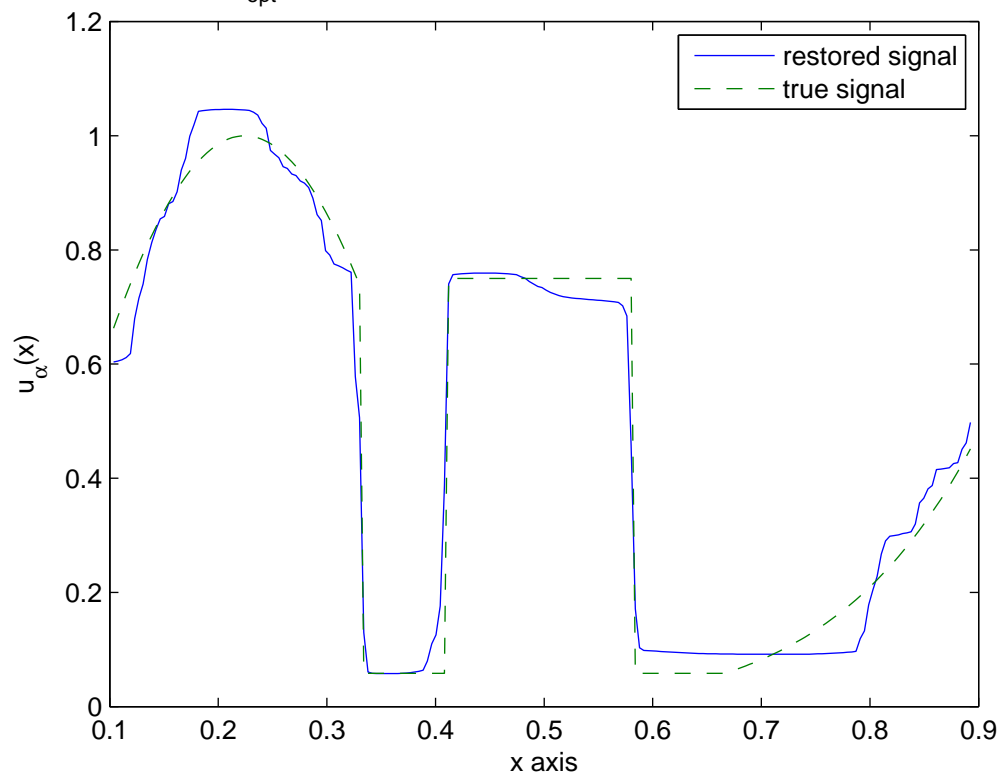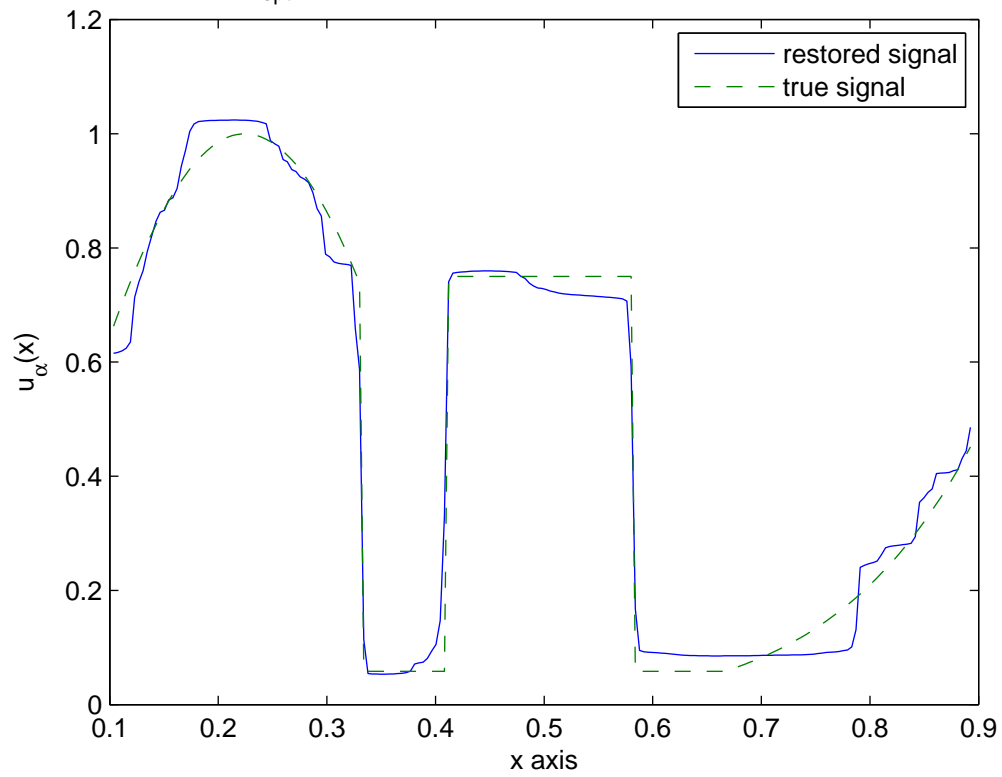α_{opt} = 0.0071969, Re. = 0.11902, Fp. = 25, It. = 19

$\alpha_{opt} = 0.0040949$, Re. = 0.091004, Fp. = 27, It. = 15

$\alpha_{opt} = 0.00233$, Re. = 0.070566, Fp. = 28, It. = 25

$\alpha_{opt} = 0.047149$, Re. = 0.2112, Fp. = 28, It. = 41